JCTC Journal of Chemical Theory and Computation

Article

pubs.acs.org/JCTC

π-Conjugation in *trans*-1,3-Butadiene: Static and Dynamical Electronic Correlations Described through Quantum Monte Carlo

Matteo Barborini[†,‡,§] and Leonardo Guidoni*[,‡]

[†]Dipartimento di Ingegneria e Scienze dell'Informazione e Matematica, Università degli studi dell'Aquila, L'Aquila, Italy

[‡]Dipartimento di Scienze Fisiche e Chimiche, Università degli studi dell'Aquila, , L'Aquila, Italy

ABSTRACT: We investigate the effects of the *static* and *dynamical electronic correlations* on the level of conjugation of the *trans*-1,3-butadiene molecule through Quantum Monte Carlo methods applied to an Antisymmetrized Geminal Power (AGP) wave function, with a Jastrow factor similar to the Gutzwiller ansatz. The degree of conjugation is measured through the convergence of the structural properties of 1,3-butadiene and in particular of the Bond Length Alternation (BLA), that is the difference between the lengths of the single and double carbon bonds. After verifying the different roles of the Fermionic AGP part of our wave function and of the Jastrow factor in recovering *electronic correlation*, we study the effects of a constrained Active Space AGP (AGP_{AS}), similar to that used in the Complete Active Space (CAS) representation. Through this AGP_{AS}, we are able to identify the effect of the limited active space on the degree of conjugation, showing that in the limit of infinite active space the structural properties converge exactly to those of the atomic AGP, giving a BLA for 1,3-butadiene around 0.1244(5) Å.

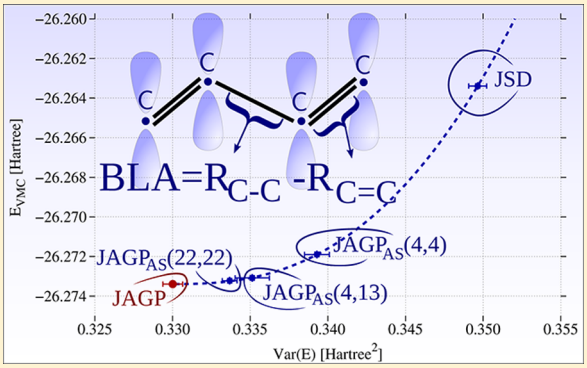

1. INTRODUCTION

π-Conjugated oligomers are an essential element in biology and in organic chemistry, often modulating charge transfer effects and energy absorption processes. Unfortunately, the description of their electronic and structural properties is a difficult task for the computational methods traditionally used in quantum chemistry, because it requires an accurate description of the combined effects of the *static* and of the *dynamical electronic correlations*. Whereas the *dynamical correlation* depends on the interaction of tight electron pairs, the *static* one depends on the presence of molecular orbitals that are degenerate or quasi-degenerate to the highest occupied ones, leading to a long-range interaction.[1]

The simplest prototype molecule for the π conjugated oligomers is *trans*-1,3-butadiene,[2−8] i.e. C_4H_6, which presents a symmetric alternation of single and double carbon bonds. The difference between the single and double carbon bonds, i.e. the Bond Length Alternation (BLA), is a quantity strictly related to the electronic properties of oligomers and polymers such as polarizabilities and electronic excitations.[1]

Experimentally, the uncertainty on the structural parameters usually obtained through Electron Diffraction (ED)[2,4−6] and Microwave Fourier Transform Spectrum (MFTS)[3] is very high, and the values predicted for the BLA spread in the range between 0.118(2)[4] and 0.146[2] Å.

A recent work reported semiexperimental values[7] for the structural properties of 1,3-butadiene in order to identify the elongation of the double bond with respect to that of ethylene. These semiexperimental results couple the experimental measurements obtained through Raman scattering, which predicted a BLA of 0.112(4) Å, with B3LYP and MP2 calculations that, as we will show later on, are unreliable in predicting the correct structures of conjugated systems. The semiexperimental value corrected through these quantum chemistry calculations was found to be equal to 0.1163(14) Å.

In general, the BLA given by the various quantum chemistry methods is around two different values of 0.115[7−12] and 0.125[13,14] Å.

Different essential ingredients are necessary to theories that aim to the accurate determination of the BLA of 1,3-butadiene, as well as the BLA of longer conjugated chains. For example, it is known that Hartree−Fock (HF) calculations do not include either *dynamical* or *static correlation*, apart from that arising from the Pauli exclusion principle. For this reason, HF tends to localize the π electrons on the double carbon bonds of butadiene, leading to an overestimation of the BLA around 0.1453 Å.[8]

Møller−Plesset (MP) perturbation theory, for π conjugated molecules, does not converge monotonically with the order of perturbation that is considered,[14] neither for the energies nor for the structural properties: moreover it is known that MP tends to delocalize the charge distributions of these conformers at least at the second perturbative order (MP2).[14−16]

Density Functional Theory (DFT) calculations are affected by the self-interaction error[17−19] that leads to the delocalization

Received: September 18, 2014
Published: January 20, 2015

DOI: 10.1021/ct501157f
J. Chem. Theory Comput. 2015, 11, 508−517

of the charge distribution, usually underestimating the BLA, at least for larger oligomer chains,[14,18] no matter if Local Density Approximation (LDA), Generalized Gradient Approximation (GGA), or hybrid functionals[20] are used. The empirically corrected functionals, that introduce the correct HF exchange in the long-range interactions, the so-called Long Range Corrected functionals (CAM-B3LYP, LC-BLYP, ωPBEh...), usually attenuate the charge delocalization but still suffer from self-interaction errors.[21]

The most accurate equilibrium structures are those obtained in ref 10 through Coupled Cluster (CC) calculations with triple perturbative excitations and different corrections, which predict a BLA of 0.1160 Å.

In this work, we investigate the effects of the *static* and *dynamical electronic correlations* through Quantum Monte Carlo (QMC) calculations, with the Jastrow Antisymmetrized Geminal Power (JAGP)[22,23] wave function based on the Resonating Valence Bond (RVB) picture introduced by Pauling to describe the chemical bonds.[24]

In quantum chemical methods like Configuration Interaction (CI), Complete Active Space (CAS), or CC, based on the multideterminantal expansion of the ground state wave function, the role of each single determinant in recovering the *static* or the *dynamical electronic correlation* is well distinguished by looking at its weight in the expansion. Usually when two or more *leading* determinants have nearly the same weight, they are said to recover *static correlation*, which is the case of diradical species[25] and multicenter metallo-organic complexes. Oppositely, in cases where many determinants are present with a rather small weight compared to the *leading* ones, these determinants are responsible for the recovering of the *dynamical electronic correlation*. Naturally, both these contributions affect the nodal surface of the ground state wave function, i.e. the multidimensional surface on which the wave function is zero. Sometimes, also a further distinction is made in the contributions to the *electronic correlation*. The so-called *nondynamical electronic correlation*, which is not considered in this article, is that related to those determinants that have low weights when describing the ground state of a given molecular system in its ground state geometry, but they become essential for the description of fragmentation processes, like in the dissociation of the H_2 molecule, for which a so-called restricted HF calculation is not *size-consistent*.

In QMC, this distinction is more subtle due to the presence of the Jastrow factor. The Jastrow factor, being a bosonic term, does not directly determine the nodal surface, but it changes the wave function through a modulation of the charge localization, and through the description of the correct electron−electron and electron−nuclei cusps conditions. Moreover, in the case of fragmentation, an appropriate Jastrow may help to suppress charge fluctuations and can be necessary to satisfy the properties of *size-consistency* and *size-extensivity*, contributing to the *nondynamical correlation*. In the present study, we will see that the Jastrow factor contributes essentially to the *dynamical correlation* of the butadiene. Our AGP fermionic part, on the other hand, is able to recover both *static* and *dynamical* contributions to the electronic correlation, and the distinction is possible by examining the weights associated with the different molecular orbitals in a JAGPn*[26] projection, as we will discuss in the following sections.

In section 2, we describe the JAGP wave function and the different representations that we will use to study the effects on the *electronic correlation*. In section 3, we discuss briefly the structural predictions of the other methods, comparing them with our QMC results. The last subsections will be devoted to the understanding of the effects of *dynamical electronic correlation* through Lattice Regularized Diffusion Monte Carlo (LRDMC) calculations and through the use of an AGP_{AS} wave function that is a constraint Antisymmetrized Geminal Power, built in a subspace of molecular orbitals similar to that used in the Complete Active Space (CAS) approach.

2. COMPUTATIONAL METHODS

The *ab initio* calculations that appear in Table 2 have been done with *NWchem 6.1.1*.[27]

2.1. Quantum Monte Carlo Methods. The QMC methods[28] are stochastic procedures to evaluate mean values of different quantum physics observables, like the energy or the atomic forces, over a given trial wave function $\Psi_T(\bar{\mathbf{x}};\{\bar{\alpha}\})$, that depends on the electronic spin and Cartesian coordinates $\bar{\mathbf{x}} = \{\mathbf{x}_1,...,\mathbf{x}_{3N}\}$ and on a set of variational parameters $\bar{\alpha}$. The parametrization $\bar{\alpha}$ of the wave function can be extremely complex and include also the direct dependence on the two-electron distances through a term called the Jastrow factor. There are different QMC methods to variationally optimize the set $\bar{\alpha}$ of parameters. In this work, we use the linear method with Hessian acceleration described in ref 29, recently improved through a new reweighting technique described in ref 30. We also optimize the structures of our molecule at the Variational Monte Carlo (VMC) level, through the methods described in refs 31 and 32 and using an optimization scheme that follows those directions which have the highest signal/noise ratio.[30,31,33]

The main drawback of QMC methods is that they are affected by stochastic errors that decrease as $1/\sqrt{\mathcal{N}}$, with the number of sampling points $\mathcal{N}$ of the electronic configuration space. On the other hand, these errors are related to the variance of the physical observables on the given trial state $\Psi_T(\bar{\mathbf{x}};\{\bar{\alpha}\})$; when this state is exactly an eigenfunction of that physical observable, the variance vanishes, giving the exact result. This *zero-variance principle* is extremely important in order to verify the quality of our approximate description of the many body problem.[30] Also, the wave functions used in QMC are able to correctly describe the electron−electron and electron−nucleus cusps conditions through the so-called Jastrow factor, recovering electronic correlation.

It has been seen that, at the Variational Monte Carlo (VMC) level, the possibility to optimize all the parameters of the variational wave function, including the exponents of the Gaussian primitives, can lead to highly accurate results even with relatively small (but optimized) basis sets.[13,25,30,32,34,35]

Furthermore, given a previously optimized trial wave function $\Psi_T(\bar{\mathbf{x}};\{\bar{\alpha}\})$, it is possible to recover all of the electronic correlation depending only on its nodal surface, through the Diffusion Monte Carlo (DMC) algorithms, like the Lattice Regularized Diffusion Monte Carlo[36] (LRDMC) used in this work.

The variational wave function used for our calculations is the Jastrow Antisymmetrized Geminal Power (JAGP),[23] built as the product of an Antisymmetric Geminal Power (AGP)[22] wave function and a Jastrow factor $J(\bar{\mathbf{r}})$, already applied in the study of different organic molecules and diradical species.[25] In the following sections, we will briefly illustrate the three representations of AGP used in our investigation, and the Jastrow factor.

DOI: 10.1021/ct501157f
J. Chem. Theory Comput. 2015, 11, 508−517

All the QMC calculations have been done with the TurboRVB[37] package from Sorella and co-workers.

2.2. Antisymmetrized Geminal Power (AGP) in the Atomic Basis. The AGP is based on the Resonating Valence Bond (RVB) representation introduced by Pauling for the description of the chemical bonds[24] and can be compared to a multideterminantal approach that considers a constraint set of molecular excitations.[23,25]

In the case of closed shell molecular systems of N_e electrons in a spin singlet state, i.e. $N_e/2 = N_e^{\uparrow} = N_e^{\downarrow}$, like 1,3-butadiene, the determinantal AGP part is written as the antisymmetrized product:

$$\Psi_{AGP}(\bar{\mathbf{x}}) = \hat{A} \prod_{i=1}^{N_e/2} \Phi_G(x_i^{\uparrow}; x_i^{\downarrow}) \tag{1}$$

of geminal functions

$$\Phi_G(\mathbf{x}_i; \mathbf{x}_j) = \sum_{a,b=1}^{M} \sum_{\mu,\nu} \lambda_{\mu_a\nu_b} \psi_{\mu_a}(\mathbf{r}_i)\psi_{\nu_b}(\mathbf{r}_j)|0, 0\rangle \tag{2}$$

defined as the linear combination of products of two atomic orbitals, of quantum numbers $\mu,\nu = (n,l,l_z)$ and centered on the ath and bth atoms, in a spin singlet state $|0,0\rangle$. The $\lambda_{\mu_a\nu_b}$ coefficients are essentially weights describing the superposition between two atomic orbitals.

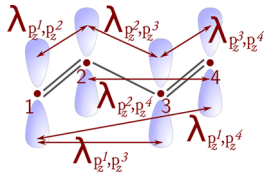

Figure 1. Scheme showing that only the coupling of the $\lambda_{i,j}$ parameters associated with the p_z orbitals which are orthogonal to the molecular plane and are responsible for the π bonding.

In Figure 1, we can see how the $\lambda_{\mu_a\nu_b}$ coefficients modulate the superposition between the p_z orbitals of the four carbon atoms in 1,3-butadiene, giving rise to the characteristic π coupling of this oligomer.

The AGP ansatz has all the appropriate *static correlation* necessary to reproduce the correct structural properties of 1,3-butadiene, because its variational space includes three particular electronic configurations: the first is the highly dimerized ground state, typical of the HF solution; the second is the resonating electronic state[31,38] in the limit of null BLA and characteristic of the metallic phase for infinite polyacetylene chains; the third is the diradical state which inverts the single and double carbon bonds in finite chains, localizing two unpaired electrons on each CH_2 ending group.[25]

2.3. AGP Projected on Molecular Orbitals. As already described in refs 25 and 26, it is possible to project the geminal expansion defined in eq 2 on a set of orthogonalized molecular orbitals built as a linear combination of the primitive orbitals that define the basis set used to create the AGP:

$$\varphi_k(\mathbf{r}) = \sum_{a=1}^{M} \sum_{\mu} c_{\mu_a}^k \psi_{\mu_a}(\mathbf{r}) \tag{3}$$

In this way, the geminal expansion becomes a sum over doubly occupied n molecular orbitals:

$$\Phi_G^{mol}(\mathbf{x}_i; \mathbf{x}_j) = \sum_{k=1}^{n} \tilde{\lambda}_{kk} \varphi_k(\mathbf{r}_i)\varphi_k(\mathbf{r}_j)|0, 0\rangle \tag{4}$$

and the projection from eq 2 to eq 4 becomes an exact mapping when n is equal to the number of atomic orbitals in the basis set. In general, this projection was introduced[26] to fasten and stabilize the convergence of the optimization procedure, and primarily to study the *dissociation* of molecules overcoming the problems of charge fluctuations present in the AGP ansatz[31,39] and that require a converged Jastrow factor to be corrected.[39]

Starting from previously optimized molecular orbitals, usually obtained by DFT calculations, these are projected on the full atomic AGP ansatz described in eqs 1 and 2. Here, the variational parameters are optimized through the linear method with a Hessian accelerator,[29] and then the wave function is projected back on the molecular orbital space defined by eqs 3 and 4.

In ref 26, it was demonstrated that the correct number of molecular orbitals n^* on which to project the atomic AGP ansatz, in order to guarantee *size-extensivity*, is equal to the number of molecular orbitals necessary to describe the dissociated noninteracting atoms. For all-electron calculations of 1,3-butadiene $n^* = 22$, while when using a pseudopotential to describe the core electrons of the carbon atoms it reduces to $n^* = 18$. When n is equal to the number of minimally occupied molecular orbitals, $n = 11$ when substituting the core electrons of the carbon atoms with pseudopotentials and $n = 15$ for all-electron calculations, we are essentially projecting the AGP expansion on a single Slater determinant (SD). In the following discussions, we will refer to this wave function as the JSD.

2.4. Active Space Molecular AGP: AGP_{AS}. In this paper, we present a further extension of the molecular AGP described through eq 4, which we can call Active Space molecular AGP (AGP_{AS}), that is built by adding to the molecular geminal expansion also the nondiagonal terms $\tilde{\lambda}_{lk}$:

$$\Phi_G^{AS}(\mathbf{x}_i; \mathbf{x}_j) = \sum_{l,k\in AS} \tilde{\lambda}_{lk} \varphi_k(\mathbf{r}_i)\varphi_l(\mathbf{r}_j)|0, 0\rangle \tag{5}$$

These terms, which couple electrons in a spin singlet state on two different molecular orbitals, must satisfy the condition $\tilde{\lambda}_{lk} = \tilde{\lambda}_{kl}$ in order to conserve the symmetry of the spatial part of the wave function with respect to the inversion of two electrons.

In this AGP_{AS} ansatz, it is possible to choose which coefficients $\tilde{\lambda}_{lk}$ to include in the Geminal expansion: these coefficients are then optimized directly with the linear optimization method.[29] Moreover, it is possible to optimize, using the same procedure, also the coefficients of the molecular orbitals defined in eq 3, but in this case, in order to avoid that the orbitals become redundant and start mixing, it is convenient to add specific constraints. These constraints can be deduced from previously optimized orbitals obtained from restricted calculations such as DFT or HF. The null coefficients of the molecular orbitals are fixed to zero, and those that appear identical in the module are imposed to be dependent by symmetry. Even though these constraints reduce the variational space, they are necessary to achieve a stable optimization without using the projection scheme described in the previous section.[26]

The great advantage of the AGP_{AS} is that it is similar to the representation of Complete Active Space (CAS). As discussed

DOI: 10.1021/ct501157f
J. Chem. Theory Comput. 2015, 11, 508−517

above, we can choose which $\tilde{\lambda}_{lk}$ coefficients to include in the Geminal expansion (eq 5) limiting the multideterminantal AGP expansion to a subset of determinants.

For example, in the case of the all-electron description of the 1,3-butadiene molecule, we have a total number of 30 electrons paired in 15 molecular orbitals. If we consider only diagonal elements with $l = k$ in the expansion with the minimum number $n = 15$ of doubly occupied molecular orbitals, we reduce again to the case of a single Slater determinant (SD), where $\tilde{\lambda}_{kk} = 1$ for $k = 1-15$. By including the LUMO and LUMO+1 orbitals, we have that $n = 17$, and we can therefore add in the Geminal expansion also the nondiagonal coefficients that couple the HOMO−1, HOMO, LUMO, and LUMO+1 orbitals, so that eq 5 will appear to be the sum of a closed shell contribution (diagonal) and a coupling determinant (active space):

$$\Phi_{\mathrm{G}}^{\mathrm{AS}}(\mathbf{x}_i; \mathbf{x}_j) = [\sum_{l=1}^{13} \tilde{\lambda}_{ll}\varphi_l(\mathbf{r}_i)\varphi_l(\mathbf{r}_j) + \sum_{l,k=14}^{17} \tilde{\lambda}_{lk}\varphi_k(\mathbf{r}_i)\varphi_l(\mathbf{r}_j)]\,|0, 0\rangle \quad (6)$$

and we will have an active space of four electrons in four orbitals (4,4) similar to the CAS(4,4) expansion.

In Figure 2, part of the $\mathrm{AGP_{AS}}$ multideterminantal expansion is reported for the (4,4) active space. Each determinant is

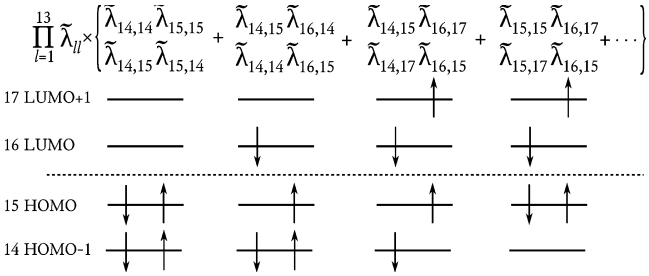

Figure 2. Partial multideterminantal expansion of the Active Space $\mathrm{AGP_{AS}}(4,4)$ wave function.

multiplied by the prefactor $\Pi_{l=1}^{13} \tilde{\lambda}_{ll}$ that is equal to 1 and that is due to the double occupied molecular orbitals that do not participate in the active space. The other two $\tilde{\lambda}_{lk}$ coefficients that multiply each determinant of the expansion depend on the electronic configuration represented by that determinant. Two important characteristics of this ansatz must be underlined. Each coefficient of the multideterminantal $\mathrm{AGP_{AS}}$ expansion is defined as the product of $N_e/2$ (N_e being the number of electrons) $\tilde{\lambda}_{lk}$ parameters, each of which contributes to the coefficients of different configurations. For this reason, unlike in the CAS method, the coefficients of the multideterminantal AGP expansion are not independent, and the $\mathrm{AGP_{AS}}$ ansatz must be considered similar to a constrained CAS expansion. Moreover, one molecular configuration can be obtained by different combinations of $\tilde{\lambda}_{lk}$ parameters, so that it will appear more than one time in the multideterminantal expansion, for example for the $\mathrm{AGP_{AS}}(4,4)$ shown in Figure 2, each configuration is represented at least by two determinants with different coefficients. Another important point that must be stressed is that because of the constraints introduced in the coefficients of the molecular orbitals to stabilize the optimization, the molecular orbitals that appear in eqs 4 and 5 can appear to be different in symmetry. The only case in which there is an exact overlap is when we limit ourselves to the SD ansatz, for which the unconstrained projected orbitals in eq 4 must be the same as those constrained by symmetry in eq 5.

In our calculations, we will consider three active spaces for 1,3-butadiene replacing the carbon atoms' core electrons with pseudopotentials. In this case, we have a total number of 22 valence electrons in 11 doubly occupied orbitals, and for this reason we consider the (22,22) active space, the (4,4) space just described, and the (4,13) space that extends the excitation of the four electrons of the HOMO−1 and HOMO orbitals to the same number of orbitals that appear in the (22,22) calculation.

To optimize these wave functions, we partially follow the procedure defined in refs 13 and 32. Starting from constrained molecular orbitals obtained by DFT or HF, we optimize the Jastrow factor, and afterwords we also relax the $\tilde{\lambda}_{lk}$ coefficients followed by those of the linear expansions in eq 3. The last step consists of the full optimization of all the wave functions' parameters, including the exponents of the primitive Gaussians.

2.5. The Jastrow Factor. The Jastrow factor[32] used in this work is similar to the Gutzwiller ansatz, used to describe the electronic correlation effects in the π conjugated polyacetylene chains.[40,41] It is written as a combination of homogeneous and nonhomogeneous terms that describe the electron−electron, electron−nuclei, and electron−electron−nuclei interactions, treating also the electron−electron and electron−nuclei cusp conditions. The nonhomogeneous three-/four-body term[32] is necessary for the correct description of dispersive interactions,[31,42] and to reduce the charge fluctuations that may appear in the AGP ansatz leading to *size extensivity* issues.[31,39]

2.6. Basis Sets. The basis sets used to build the AGP and SD wave functions for the all-electron calculations are a mixture of Gaussian and Slater type orbitals (Table 1). For the carbon

Table 1. Basis Sets Used for the Quantum Monte Carlo Calculations

	carbon atom	hydrogen atom
all-electron basis sets		
atomic basis sets		
GTO[a]	(9s5p2d)/[4s3p2d]	(4s1p)/[2s1p]
STO[b]	(1s1p1d)	(1s1p)
Jastrow basis sets		
GTO[c]	(4s3p2d)	(2s1p)
ECP[d] basis sets		
atomic basis sets		
1[a]	(4s4p)/[2s2p]	(3s3p)/[1s1p]
2[a]	(5s5p2d)/[3s2p1d]	(4s3p)/[2s1p]
Jastrow basis sets		
1[a]	(4s3p)/[2s2p]	(3s2p)/[1s1p]
2[a]	(4s3p2d)/[3s2p1d]	(3s2p)/[2s1p]
3[a]	(5s4p3d)/[4s3p2d]	(3s2p)/[2s1p]

[a]Contracted Gaussian type orbitals. [b]Uncontracted Slater type orbitals. [c]Uncontracted Gaussian type orbitals. [d]Energy consistent pseudopotential with relativistic corrections.[43]

atoms, we use (9s5p2d)/[4s3p2d] Gaussian contracted orbitals with (1s1p1d) uncontracted Slater type ones, while for the hydrogen atoms we use (4s1p)/[2s1p] contracted Gaussian orbitals with (1s1p) uncontracted Slater type ones. The basis set for the Jastrow factor is built as a combination of uncontracted Gaussian orbitals: (4s3p2d) for the carbon atoms and (2s1p) for the hydrogen atoms. For the pseudopotential calculations, we used the energy-consistent

DOI: 10.1021/ct501157f
J. Chem. Theory Comput. 2015, 11, 508−517

pseudopotential with relativistic corrections[43] (ECP) only for the carbon atoms.

For these calculations, we have used different Gaussian contracted basis sets for both the fermionic part of the wave function, the AGP or SD, and for the Jastrow bosonic part. All the basis sets are summarized in Table 1.

3. RESULTS AND DISCUSSIONS

3.1. Bond Length Alternation of 1,3-Butadiene: General Results. As discussed in the Introduction, quantum chemistry methods predict two possible values of the BLA around 0.115[7−12] and 0.125[13,14] Å, the latter obtained also by our VMC calculations published in a previous paper[13] and partially reported in Table 2. To understand which one of these two values of the BLA is the most reliable, we must first discuss the various results, summarized in Table 2, with respect to the intrinsic errors of each computational method.

Table 2. Geometries of *trans*-1,3-Butadiene

	$R_{C=C}$ [Å]	R_{C-C} [Å]	BLA [Å]
J_1AGP_1 (ECP)[a]	1.3326(2)	1.4583(4)	0.1257(4)
CASSCF[b]	1.345	1.463	0.118
RASSCF[b]	1.351	1.468	0.117
CASSCF[c]	1.344	1.467	0.123
CASPT2[c]	1.348	1.454	0.106
HF[d]	1.3225	1.4676	0.1450
CISD[d]	1.3316	1.4631	0.1315
CISDT[d]	1.3340	1.4627	0.1287
CCSD(T)/CBS[e]	1.3389	1.4549	0.1160
CCSD[d]	1.3429	1.4663	0.1234
CCSD(T)[d]	1.3494	1.4648	0.1154
CCSDT[d]	1.3496	1.4648	0.1151
$CCSDT(2)_Q$[d]	1.3500	1.4646	0.1146
QCISD[d]	1.3436	1.4664	0.1229
QCISD(T)[d]	1.3503	1.4650	0.1147
MP2[c]	1.343	1.456	0.113
MP2[f]	1.3401	1.4533	0.1132
MP2[g]	1.3425	1.4562	0.1137
MP2[d]	1.3440	1.4578	0.1138
MP3[d]	1.3396	1.4646	0.1250
MP4(SDQ)[o]			0.1227
MP4(SDTQ)[d]	1.3493	1.4639	0.1146
B3LYP[c]	1.339	1.456	0.117
B3LYP[f]	1.3339	1.4527	0.1188
B3LYP[h]	1.3344	1.4527	0.1183
CAM-B3LYP[d]	1.3328	1.4595	0.1267
Semi-Exp[i]	1.3376(10)	1.4539(10)	0.1163(14)
SED[j]	1.3439(5)	1.4672(13)	0.1233(14)
ED[k]	1.341(2)	1.463(3)	0.122(3)
ED[l]	1.349(1)	1.467(2)	0.118(2)
MFTS[m]	1.337	1.467	0.130
ED[n]	1.337	1.483	0.146

[a]Variational Monte Carlo results from ref 13. [b]CASSCF(4,8)/6-31G*+3p and RASSCF(22,9 + 5+12)[1,1]/6-31G*+3p are taken from ref 9. [c]Calculations with 6-31G* basis set from ref 44. [d]This work, with the 6-31G* basis set. [e]CCSD(T)/CBS calculations with various corrections from ref 10. [f]Calculations with the cc-pVTZ basis set from ref 7. [g]Calculations with 6-31G* basis set from ref 12. [h]Calculations with auc-cc-pVTZ basis set from ref 11. [i]Semiexperimental results from ref 7. [j]Selection electron diffraction from ref 6. [k]Electron diffraction from ref 5. [l]Electron diffraction from ref 4. [m]Microwave Fourier transform spectrum from ref 3. [n]Electron diffraction from ref 2. [o]Calculations from ref 14 with the 6-31G* basis set.

As already anticipated in the Introduction, HF calculations, which do not include electronic correlation, tend to localize[8] the π conjugated electrons around the double bonds, leading to an overdimerized structure. The BLA predicted by MP perturbation theory does not converge monotonically with the perturbative orders that are considered. As a matter of fact, with the 6-31G* basis set, the MP3 and MP4(SDQ) calculations predict a BLA between 0.1250 and 0.1227[14] Å, while MP2 and MP4(SDTQ) give values of 0.1138 and 0.1146 Å, respectively. These inconsistent results show that the effects of the third and forth perturbative orders are comparable in size, and they cancel out in the expansion. For these reasons, MP calculations cannot be considered as a reliable reference for the structural properties of π conjugated oligomers. The problems of DFT in describing the π conjugation are due to the charge delocalization that leads to an underestimation of the BLA that is independent of the exchange correlation functional used.[14,17,18,18,19]

How these errors act on 1,3-butadiene is unknown, but we can see that while the BLA predicted with the B3LYP exchange correlation functional[7,11,44] is between 0.117 and 0.1188 Å, that obtained with its long-range corrected counterpart, the CAM-B3LYP[45] functional, is predicted to be around 0.1267 Å with the 6-31G* basis set. Finally, we are left with the *ab initio* structures obtained with Configuration Interaction (CI), Quadratic Configuration Interaction (QCI), and Coupled Cluster (CC). Of the three, the only method which is *variational* but not *size-extensive*, CI, gives a different value of the BLA with respect to QCI and CC, around 0.1287 Å when including triple excitations. Because it is clear that the value of the BLA for CI is still not converged at the CISDT level, nothing can be clearly predicted, even if it seems to be converging toward the value of 0.125 Å obtained also through our VMC calculations. The behaviors of CC and QCI with respect to the excitations included in the calculation are identical, and when triple excitations are included, the BLA obtained is respectively of 0.1154 and 0.1147 Å. The difference between CI and CC (or QCI) could depend on two computational aspects: the first is that CC recovers more *dynamical correlation* with respect to CI; the second is that the property of *size-extensivity*, which CI fails to respect, could be quite important for conjugated systems.

For this reason, the only accurate structures that we can consider as a reference, and to which we can compare our QMC calculations, are those obtained with CCSD(T)/CBS calculations in ref 10, which predict a shorter BLA of 0.1160 Å.

3.2. The Role of the AGP Ansatz on the *Electronic Correlation* of 1,3-Butadiene. To make a comparison between our VMC structures and that obtained through CCSD(T)/CBS,[10] it is essential to clarify the stability of the VMC results. For this purpose, we have done different calculations with the basis sets described in Table 1, and with the atomic JAGP and the molecular JSD ansätze described in the Computational Methods. All of the results are reported in Table 3.

The first effect can be seen by comparing the differences in the structures obtained with the SD and AGP ansätze. The BLA given by the two is essentially the same, but the AGP gives an elongation of both the carbon bonds of 0.002 Å with respect to the SD, as already pointed out in two previous works.[13,32] The effect of the substitution of the core electrons with the ECP

DOI: 10.1021/ct501157f
J. Chem. Theory Comput. 2015, 11, 508−517

Table 3. Geometries of *trans*-1,3-Butadiene Obtained with VMC Calculations[a]

	single determinant				antisymmetrized geminal power			
	$R_{C=C}$ [Å]	R_{C-C} [Å]	BLA [Å]	E [Hartree]	$R_{C=C}$ [Å]	R_{C-C} [Å]	BLA [Å]	E [Hartree]
all-electron	1.3318(5)	1.4585(8)	0.1267(10)	−155.8857(2)	1.3345(5)	1.4593(8)	0.1247(10)	−155.8962(2)
J_1 w.f.$_1$ (ECP)					1.3326(2)	1.4583(4)	0.1257(4)	−26.2686(1)
J_1 w.f.$_2$ (ECP)	1.3309(2)	1.4554(4)	0.1246(4)	−26.2587(1)	1.3323(2)	1.4582(4)	0.1259(4)	−26.2691(1)
J_2 w.f.$_2$ (ECP)	1.3304(3)	1.4565(5)	0.1261(6)	−26.2632(1)	1.3326(3)	1.4577(5)	0.1251(6)	−26.2730(1)
J_3 w.f.$_2$ (ECP)	1.3301(3)	1.4558(5)	0.1257(6)	−26.2635(1)	1.3328(2)	1.4572(5)	0.1244(5)	−26.2734(1)

[a]The basis sets used to obtain the VMC structures with all-electron (AE) and pseudopotential (ECP) approaches, and with the JAGP and JSD ansätze, are described in Table 1. We indicate with J_i the basis set used for the jastrow factor, while with w.f.$_i$ the one used for the Fermionic part of the wave function.

pseudopotentials, which can be seen by comparing the structures of the JAGP (AE) wave function with those of the J_3AGP_2 (ECP) one, is a contraction of both the bonds of nearly 0.002 Å with respect to the AE calculations.[32]

Another important issue that must be verified in order to establish the quality of the VMC results is the presence of possible charge fluctuations in the JAGP ansatz which lead to problems of *size-extensivity*.[29,39] To verify this effect that could be the reason for the small discrepancy in the BLAs shown for SD and AGP in Table 3, we have done different structural optimizations using the AGP_2 and SD_2 wave functions and different $J_{1,2,3}$ Jastrow factors (Table 3). By comparing these results, we can see that the effect of the Jastrow on the convergence of the structural parameters is very small for both the JSD and JAGP wave functions. While for the single determinant ansatz the Jastrow tends to slowly elongate the bonds, for the AGP ansatz the effect of the Jastrow seems opposite. Moreover, for the JSD, the largest Jastrow factor tends to elongate the BLA, converging towards a value between 0.1261(11) and 0.1257(10) Å, at variance with the results obtained with the J_1AGP_1 and J_1AGP_2 wave functions. Despite these small variations, the values of the BLA predicted by VMC are solidly between 0.124(1) and 0.126(1) Å, and we can conclude that the effect of possible charge fluctuations in the AGP ansatz is negligible. The difference in the bond lengths between the JSD and JAGP ansätze is therefore dependent on the correlation recovered by the AGP multideterminantal expansion. To assign this effect to a *dynamical* or *static contribution*, we have projected the fermionic AGP part of the optimized J_1AGP_2, J_2AGP_2, and J_3AGP_2 wave functions on the diagonalized molecular expansion JAGPn*, with n* = 22 molecular orbitals, described in eq 4.

The ratio between the coefficient associated with the HOMO orbital and those related to the unoccupied LUMO+k ones are plotted in Figure 3. From these results, it appears that the coefficients of the two different fermionic basis sets, AGP_1 and AGP_2, with the same J_1 Jastrow factor, have different expansions and that the greatest discrepancy is in the weights associated with the LUMO and LUMO+1 orbitals. On the other hand, within the same AGP_2 basis set, the effect of increasing the Jastrow factor is only that of remodulating the amplitudes of the LUMO+k coefficients that appear to be nearly converged with the J_2 and J_3 Jastrow factors. Naturally, the expansion is dominated by a single Slater determinant, as expected by the chemistry of these insulating systems, and the LUMO and LUMO+1 orbitals have very small weights with respect to the HOMO one, contributing respectively of about 8% and 4% in the AGP expansion. For this reason, we can conclude that the multideterminantal expansion is recovering essentially *dynamical correlation*, modifying the nodes of the wave function in a

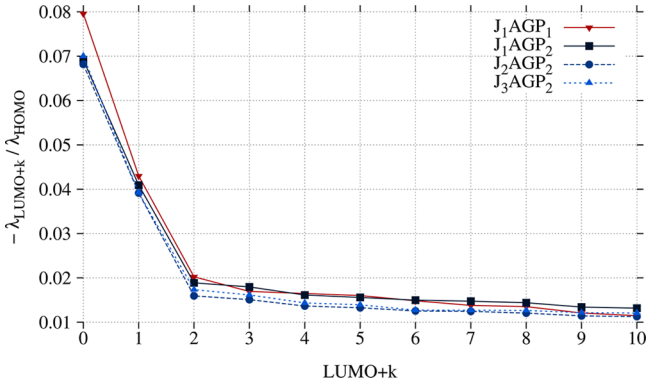

Figure 3. $\lambda_{LUMO+k}/\lambda_{HOMO}$ ratio of the coefficients of the geminal expansion described in eq 4 and obtained by diagonalizing the JAGP wave functions built with the different basis sets and Jastrow factors.

way that is not achievable by the JSD ansatz. The effect ascribed to the *dynamical correlation* recovered by the AGP is that of elongating both the carbon bond lengths, without changing the degree of conjugation.

3.3. $JAGP_{AS}$ Applied to 1,3-Butadiene: BLA's Dependency on Molecular Configurations. To verify the effects of the *electronic correlation* recovered by the multideterminantal AGP ansatz on the structural parameters, here we use the active space $JAGP_{AS}$ described in the previous section. Through this reduced ansatz, it is possible to select the coupling of the molecular orbitals, including only some excitations in the expansion. To understand the effect of this molecular coupling, we have chosen as starting points for the optimizations three different sets of molecular orbitals on their optimized structures, all built from the uncontraction of the AGP_2 basis set with the addition of the J_3 Jastrow factor (Table 1). We considered HF molecular orbitals on the HF structure, which is the case of high dimerization, B3LYP orbitals on B3LYP structures that delocalize the charge and give a BLA similar to that of CCSD(T)/CBS, and the molecular orbitals obtained through the projection of the atomic J_3AGP_2 on the diagonalized molecular expansion described in eq 4, with n = 22. Fixing the symmetries in the molecular orbitals, as described in the previous section, full wave function optimizations followed by structural optimizations were carried out for the SD wave function, and for the AGP_{AS} with three different active spaces (4,4), (4,13), and (22,22). These results are reported in Table 4.

It can be observed that the optimized results obtained starting from the HF and B3LYP orbitals and structures are identical. The two opposite cases converge to the same structural and energetic result depending only on the active

DOI: 10.1021/ct501157f
J. Chem. Theory Comput. 2015, 11, 508−517

Table 4. Structures and Energies of *trans*-1,3-Butadiene with the $JAGP_{AS}$ Wave Function, Compared with the JAGP[a]

	$R_{C=C}$ [Å]	R_{C-C} [Å]	BLA [Å]	E [Hartree]
from HF orbitals and structures				
JSD	1.3307(4)	1.4561(7)	0.1254(8)	−26.2636(1)
$JAGP_{AS}(4,4)$	1.3339(3)	1.4508(7)	0.1168(8)	−26.2699(1)
$JAGP_{AS}(4,13)$	1.3327(3)	1.4551(4)	0.1224(5)	−26.2732(1)
$JAGP_{AS}(22,22)$	1.3330(3)	1.4557(4)	0.1227(5)	−26.2733(1)
from B3LYP orbitals and structures				
JSD	1.3302(2)	1.4549(6)	0.1247(6)	−26.2637(1)
$JAGP_{AS}(4,4)$	1.3341(2)	1.4502(6)	0.1161(6)	−26.2699(1)
$JAGP_{AS}(4,13)$	1.3330(3)	1.4555(5)	0.1225(6)	−26.2732(1)
$JAGP_{AS}(22,22)$	1.3327(4)	1.4553(5)	0.1226(6)	−26.2732(1)
from JAGP projected orbitals and structures				
JSD	1.3305(3)	1.4556(6)	0.1251(7)	−26.2634(1)
$JAGP_{AS}(4,4)$	1.3335(3)	1.4537(9)	0.1202(9)	−26.2719(1)
$JAGP_{AS}(4,13)$	1.3328(3)	1.4560(4)	0.1232(5)	−26.2732(1)
$JAGP_{AS}(22,22)$	1.3329(3)	1.4560(5)	0.1231(6)	−26.2731(1)
JAGP reference				
J_3AGP_2	1.3328(3)	1.4572(5)	0.1244(6)	−26.2734(1)

[a]All the calculations have been done with the same basis set used for the J_3AGP_2 wave function, described in Table 1.

space that has been considered. The results obtained starting from the projected JAGP molecular orbitals are slightly different for the smallest active spaces, because of the fact that they are slightly "rotated" in the Hilbert space with respect to those given by HF and B3LYP calculations.

For the SD, $AGP_{AS}(4,13)$, and $AGP_{AS}(22,22)$ active spaces, the three starting points always converge to results that are at variance between each other, and, as the active space grows, the structural properties and the energies converge to the variational result given by the atomic J_3AGP_2 wave function reported in the last line of Table 4.

The interesting and surprising result is that obtained for the $AGP_{AS}(4,4)$ wave function. In this subset, the HF and B3LYP starting points converge to the same result, which has a reduced BLA between 0.1161(6) and 0.1168(8) Å, similar to that of CCSD(T)/CBS, due principally to the reduction of the single bond and second to a small elongation of the double one, with respect to the $AGP_{AS}(4,13)$, $AGP_{AS}(22,22)$, and the atomic AGP wave functions.

This suggests that the result given by $AGP_{AS}(4,4)$, higher in energy, is simply wrong and depends on the limitation of the active space.

In Figure 4, the energies of the SD and of the different AGP_{AS} active spaces, for the three different starting functions, are reported with respect to their variance. For the *zero-variance principle*, the ansatz associated with the lowest variance is the most accurate. We can see that the $JAGP_{AS}(4,4)$ results are intermediate between the JSD and the $JAGP_{AS}(4,13)$ calculations, while the most converged result with lower variance is that obtained for the atomic JAGP wave function that naturally contains all the variational $JAGP_{AS}(n,n)$ subspaces.

In conclusion, this ansatz favors variationally the value of 0.1244(6) Å for the BLA, with respect to that of 0.1161(6) Å, also obtained through CCSD(T), QCISD(T), MP2, and MP4.

3.4. Comparison between CCSD(T) and JAGP Molecular Structures. *3.4.1. Dynamical Correlation.* Having verified the convergence of the VMC calculations, the way in which the JAGP ansatz recovers *dynamical correlation*, and the

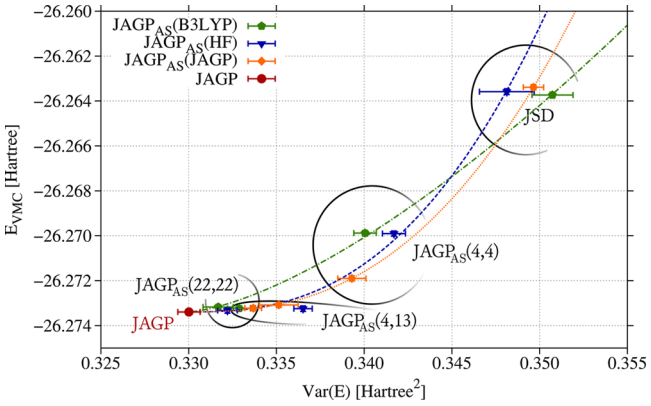

Figure 4. Energy as a function of the variance for the different $JAGP_{AS}$ and starting from the three sets of molecular orbitals and structures: the highly dimerized HF, the delocalized B3LYP, and the orbitals obtained from the projected atomic JAGP.

limitation of the active space on conjugation, the reason for the difference of 0.01 Å between the BLAs of the CCSD(T)/CBS and JAGP ansätze is still unclear.

The fact that this difference is also registered between the CCSD and CCSD(T) (CCSDT, $CCSDT(2)_Q$) calculations, and between the QCISD and QCISD(T) ones, may lead to the hypothesis that the CCSD, QCISD, and JAGP ansätze are still missing *dynamical electronic correlation*. Unfortunately, it is impossible to clearly identify which determinants, of the higher order excitations, are responsible for the different BLAs. For example, the T excitations are present in the CISDT, QCISD(T), CCSD(T), and CCSDT calculations reported in Table 1, and they give different results. The change in the conjugation may be due to a compensating effect of the T and Q excitations (some of which are present in the QCISD(T), CCSD(T), and CCSDT ansätze), but this could be demonstrated only through a CISDTQ calculation which is at present computationally prohibitive.

In order to verify how the *dynamical correlation* treated by the JAGP ansatz selects between the CCSD(T)/CBS and JAGP converged structures, we compared the JAGP all-electron wave function on the JAGP all-electron equilibrium geometry ($JAGP_{JAGP}$), reported in Table 3, with the JAGP wave function optimized on the CCSD(T)/CBS structure reported in ref 10 ($JAGP_{CCSD(T)/CBS}$), doing both VMC and Lattice Regularized Diffusion Monte Carlo (LRDMC) energy calculations (Table 5).

Table 5. Quantum Monte Carlo Energies of *trans*-1,3-Butadiene on the All-Electron Optimized Structures Obtained through JAGP[a] and CCSD(T)/CBS[b] Calculations

		$JAGP_{CCSD(T)/CBS}$ [Hartree]	$JAGP_{JAGP}$ [Hartree]	ΔE [eV]
VMC		−155.8947(2)	−155.8961(2)	0.038(8)
LRDMC	$a = 0.20$	−155.9669(2)	−155.9699(2)	0.081(8)
	$a = 0.15$	−155.9644(2)	−155.9667(2)	0.062(8)
	$a = 0.10$	−155.9616(3)	−155.9635(3)	0.052(11)
	$a = 0.05$	−155.9594(3)	−155.9605(3)	0.030(11)
	$a \rightarrow 0$	−155.9585(3)	−155.9596(3)	0.030(11)

[a]JAGP (AE) structure reported in Table 3. [b]Structure obtained with coupled cluster calculations in the complete basis set (CBS) limit with various corrections from ref 10.

DOI: 10.1021/ct501157f
J. Chem. Theory Comput. 2015, 11, 508−517

The LRDMC calculations on the two different structures are obtained, by extrapolating to the continuum limit ($a \to 0$), through the function $E(a) = E_{a\to 0} + Aa^2 + Ba^4$, the energies of different space discretizations $a \in \{0.05, 0.10, 0.15, 0.20\}$ [au] (Figure 5) reported in Table 5.

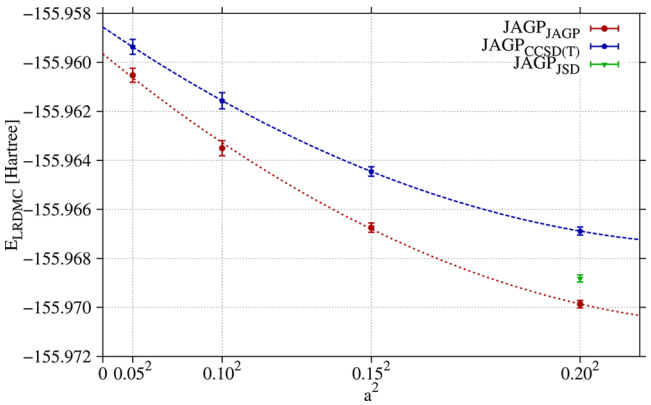

Figure 5. Fitting of the LRDMC energies as a function of the square of the lattice space a^2, with the function $E(a) = E_{a\to 0} + Aa^2 + Ba^4$.

In Figure 5, we also report the value of the LRDMC energy, for $a = 0.20$ au, of an optimized JAGP wave function on the JSD (AE) structure reported in Table 3. It is evident, by the results in Table 5 and Figure 5, that the JAGP structure is constantly lower in energy with respect to the CCSD(T)/CBS one, with a difference of 0.030(11) eV in the limit $a \to 0$ that is at variance with the difference found at the VMC level (of 0.038(8) eV).

The fact that the energy difference is conserved at both the VMC and LRDMC level demonstrates that the *dynamical correlation* of the JAGP favors the JAGP structure, and so does its nodal surface. Moreover, the JSD structure is more compatible with the nodal surface given by the JAGP ansatz, with respect to that of the CCSD(T)/CBS calculations. Unfortunately, these results are still unable to identify the best structural parameters between those predicted by the JAGP and CCSD(T)/CBS ansätze, nor are they able to justify the differences.

3.4.2. Molecular Fragmentation and Size-Consistency. The last issues that we want to analyze are the property of *size-consistency* and the ability of the various ansätze to properly describe the molecular fragmentation without introducing any kind of spin contamination. In the case of the breaking of the single or double bonds of 1,3-butadiene, none of the methods reported in Table 1, and based on restricted single references, can properly describe the molecular fragmentations, not even CCSD(T).[46,47]

To understand if the JAGP and CCSD(T) ansätze treat the two carbon bonds of 1,3-butadiene in a different way, we decided to study the elongation (contraction) of the double bond (single bond) between 1,3-butadiene and the prototype molecule for that particular bond, i.e. ethylene (ethane). In the breaking of the single bond, Figure 6b, we can observe that the molecule dissociates in two $C_2H_3^{\bullet}$ fragments both with one unpaired electron. In this case, the JAGP wave function is able to correctly describe the molecular fragmentation, as for the case of the dissociation of the H_2 molecule, because it is able to correctly describe the spin localization on the two fragments, also conserving the spin state $S(S + 1) = 0$ ($S_z = 0$) (no spin

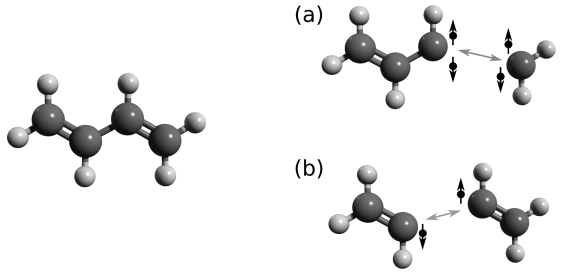

Figure 6. Dissociation of the double (a) and single (b) bonds of the 1,3-butadiene molecule with the JAGP ansatz.

contamination, unlike unrestricted calculations) during all the dissociation process. However, in the breaking of the double bond, Figure 6a, the AGP behaves like all the other methods based on restricted SD references, reported in Table 2, conserving $S_z = 0$ and $S(S + 1) = 0$, and leading to the production of a methylene molecule in its excited singlet state[25] and a C_3H_4 residue which is in an unstable electronic and structural configuration. This means that the JAGP ansatz is unable to properly describe the breaking of the double bond. Apart from the asymmetric behavior of the JAGP in describing the fragmentations of the two molecular bonds, the problem of *size-consistency* remains. As a matter of fact, the charge fluctuations present in the JAGP can lead, even in the case of the breaking of the single bond, to an error in the estimation of the dissociation energies. We must stress here that these errors are not so dramatic, as seen in the study of the dissociation curves of the triplet state of the O_2 molecule (in the appendix of ref 48) and in that of the water dimer (in refs 35 and 42).

In order to verify the possible effects of this inhomogeneous behavior of the JAGP in describing molecular fragmentation, in Table 6 we compare the structures of C_2H_4 and C_2H_6 obtained through VMC calculations on the JAGP all-electron ansatz,

Table 6. Geometries of the C_2H_4 and C_2H_6 Molecules[a]

	R_{CC} [Å]	R_{CH} [Å]	θ_{HCH} [deg]
	ethane		
JAGP	1.5262(2)	1.0879(2)	111.29(2)
CCSD(T)[i]	1.5240	1.0895	111.23
CCSD(T)[b]	1.5227	1.0890	111.23
ED[c]	1.531(2)	1.095(2)	111.5(3)
ED[l]	1.524	1.089	
IMS[l]	1.528_0	1.087_7	
	ethylene		
JAGP	1.3304(2)	1.0796(2)	117.06(2)
CCSD(T)[d]	1.3307	1.0809	117.12
Exp[e]	1.3370	1.0860	117.62
ED[f]	1.330(5)	1.079(5)	
IR[g]	1.334(2)	1.081(2)	117.36(17)
MW[h]	1.339	1.085	117.8

[a]The VMC results are obtained through all-electron JAGP wave functions with the mixed Gaussian/Slater basis set described in Table 1. [b]CBS results from ref 49. [c]Corrected results from electron diffraction, ref 50. [d]Complete basis set convergence, with various corrections from ref 51. [e]Experimental data from ref 52. [f]Electron diffraction from ref 53. [g]From infrared and Raman vibrational constants, ref 54. [h]Microwave results from ref 55. [i]CBS results from reg 56. [l]Electron diffraction and infrared and microwave spectroscopy from ref 57. The authors report a probable uncertainty of 0.005 Å on the CH bond and of 0.003 Å on the CC bond.

DOI: 10.1021/ct501157f
J. Chem. Theory Comput. 2015, 11, 508−517

with those obtained through CCSD(T)/CBS calculations, also reporting different experimental values.

We can see that the double bonds predicted in C_2H_4 with the CCSD(T)/CBS and JAGP ansätze are identical within the error bars. The single bond obtained with the JAGP for C_2H_6, on the other hand, is more compatible with the experimental one, 0.005 Å longer then that predicted by CCSD(T).

By observing the elongation (contraction) of the double (single) bond between that of the 1,3-butadiene and that of the C_2H_4 (C_2H_6) molecule, we can see that the elongation of the double bond between C_2H_4 and C_4H_6 is for CCSD(T) about 0.0082 Å, while in VMC it is exactly half that value, 0.0041 Å; for both JAGP and CCSD(T), the compression of the single bond is absolutely comparable, around 0.0678 and 0.0669 Å for the two ansätze, respectively.

In conclusion, the discrepancy of 0.01 Å between the BLA obtained by VMC and that obtained with CCSD(T)/CBS calculations is the result of two comparable effects: the single bond length predicted by VMC in C_2H_6 is 0.002/0.004 Å longer than the one obtained with CCSD(T)/CBS; this discrepancy is conserved also in butadiene. The double bonds predicted by VMC and CCSD(T) in C_2H_4 are identical but in butadiene CCSD(T)/CBS gives a larger elongation, of 0.004 Å. Still, these results are unable to clearly explain the differences between the BLAs of the CCSD(T) and JAGP ansätze, assigning them to the property of *size-consistency* or to the ability to describe molecular fragmentation.

4. CONCLUSIONS

To understand the necessary ingredients to describe correctly the π conjugation of conjugated organic chains, like polyacetylene fragments, we have studied the convergence of the Bond Length Alternation (BLA) of the *trans*-1,3-butadiene, which is a prototype molecule for these systems, with the Variational Monte Carlo (VMC) method applied to the Jastrow Antisymmetrized Geminal Power (JAGP) wave function.

Through the Lattice Regularized Diffusion Monte Carlo (LRDMC) method, we have confirmed that the BLA predicted by the JAGP ansatz must be 0.1244(6) Å, slightly smaller than that obtained with a single determinant JSD wave function of 0.1257(6)Å.

In order to understand how the degree of conjugation depends on the multiconfigurational AGP expansion, which contributes to the *dynamical correlation*, we have defined a constraint AGP in the molecular space, the AGP_{AS}, studying the convergence of the structural properties starting from three different wave functions and from different structures. We started from molecular orbitals and structures obtained by HF theory, which is the case of high dimerization; by Density Functional Theory with the B3LYP exchange-correlation functional, which gives a charge delocalization; and through the projection of the atomic JAGP on the molecular subspace.

From the molecular and structural starting points of the HF and B3LYP calculations, constraining the active space to (4,4), we have obtained a value for the BLA between 0.1161(6) and 0.1168(8) Å, respectively. In particular, this shorter value of the BLA predicted by the reduced AGP_{AS} is due to the shortening of the single bond of about 0.007 Å with respect to that of the JAGP. Through the calculations in Table 4, it is evident that the bond which is most affected by the change in the active space is the single carbon bond. Probably the nonuniform inclusion of the excitations in the (4,4) space is at the origin of this erroneous behavior. When the complete active space grows to include a larger set of molecular excitations, the BLA converges to the atomic JAGP value of 0.1244(6) Å, definitely confirming our previously calculated value.[13]

The discrepancy found between the CCSD(T)/CBS (or QCISD(T)) value of the BLA of 0.1160 Å and that predicted by all our JAGP and JSD VMC calculations remains unexplained. We must remember here that the ability of the JAGP ansatz to describe the resonating state, in which the lengths of the single and double carbon bonds coincide, should favor the charge delocalization and so the shortening of the BLA.

The fact that the BLA obtained by JAGP is similar to the BLA obtained by the JSD ansatz, and that the AGP multideterminant expansion affects only the absolute length of the carbon bonds but not their difference, leaves us with two hypotheses. The first is that the CCSD(T) (or QCISD(T)) multideterminantal ansatz recovers more *dynamical correlation* than the JSD and JAGP ansätze. If this is the case, then the *dynamical correlation* missed by our ansätze might be responsible for the changes in the description of the degree of conjugation. The second hypothesis is that the discrepancy may arise from the fact that CC and QCI include the molecular configurations related to the excited states in a nonlinear way, at variance with the CISD and CISDT expansions. This might be important for the BLA's convergence as a function of the order of the excited state configurations introduced. CISD and CISDT methods, which introduce the configurations of the excited states in a linear way, seem indeed to converge to our JAGP results. From a perspective, only additional calculations of higher accuracy but with a linear inclusion of excitations, such as CISDTQ, may in the future unequivocally clarify which of the above-mentioned hypotheses is valid.

AUTHOR INFORMATION

Corresponding Author

*E-mail: leonardo.guidoni@univaq.it.

Present Address

[§]CNR - Istituto di Nanoscienze, S3 Research Center, Via Campi 213/a, 41125 Modena, Italy.

Notes

The authors declare no competing financial interest.

ACKNOWLEDGMENTS

The authors thank Daniele Varsano, Andrea Zen, and Emanuele Coccia for stimulating discussions and critical considerations. The authors acknowledge funding provided by the European Research Council, project no. 240624 within the VII Framework Program of the European Union. Computational resources were supplied by CINECA, PRACE infrastructure, and the Caliban-HPC centre at the University of L'Aquila.

REFERENCES

(1) Choi, C. H.; Kertesz, M.; Karpfen, A. *J. Chem. Phys.* **1997**, *107*, 6712−6721.

(2) Almenningen, A.; Bastiansen, O.; Traetteberg, M. *Acta Chem. Scand.* **1958**, *12*, 1221.

(3) Caminati, W.; Grassi, G.; Bauder, A. *Chem. Phys. Lett.* **1988**, *148*, 13.

(4) Kveseth, K.; Seip, R.; Kohl, D. A. *Acta Chem. Scand. Ser. A* **1980**, *34*, 31.

(5) Kuchitsu, K.; Fukuyama, T.; Morino, Y. *J. Mol. Struct.* **1968**, *1*, 463−479.

DOI: 10.1021/ct501157f
J. Chem. Theory Comput. 2015, 11, 508−517

(6) Haugen, W.; Trætteberg, M. *Acta Chem. Scand.* **1966**, *20*, 1726−1728.
(7) Craig, N. C.; Groner, P.; McKean, D. C. *J. Phys. Chem. A* **2006**, *110*, 7461−7469.
(8) Fogarasi, G.; Liu, R.; Pulay, P. *J. Phys. Chem.* **1993**, *97*, 4036−4043.
(9) Boggio-Pasqua, M.; Bearpark, M. J.; Klene, M.; Robb, M. A. *J. Chem. Phys.* **2004**, *120*, 7849−7860.
(10) Feller, D.; Craig, N. C. *J. Phys. Chem. A* **2009**, *113*, 1601−1607.
(11) McKean, D. C.; Craig, N. C.; Panchenko, Y. N. *J. Phys. Chem. A* **2006**, *110*, 8044−8059.
(12) Panchenko, Y.; Auwera, J.; Moussaoui, Y.; De Mar, G. *Struct. Chem.* **2003**, *14*, 337−348.
(13) Barborini, M.; Guidoni, L. *J. Chem. Phys.* **2012**, *137*, 224309.
(14) Jacquemin, D.; Perpète, E. A.; Ciofini, I.; Adamo, C. *Chem. Phys. Lett.* **2005**, *405*, 376−381.
(15) Hirata, S.; Torii, H.; Tasumi, M. *J. Chem. Phys.* **1995**, *103*, 8964−8979.
(16) Jacquemin, D.; Adamo, C. *J. Chem. Theory Comput.* **2011**, *7*, 369−376.
(17) Varsano, D.; Marini, A.; Rubio, A. *Phys. Rev. Lett.* **2008**, *101*, 1−4.
(18) Ciofini, I.; Adamo, C.; Chermette, H. *J. Chem. Phys.* **2005**, *123*, 121102.
(19) Körzdörfer, T.; Parrish, R. M.; Sears, J. S.; Sherrill, C. D.; Brédas, J.-L. *J. Chem. Phys.* **2012**, *137*, 124305.
(20) Jacquemin, D.; Femenias, A.; Chermette, H.; Ciofini, I.; Adamo, C.; André, J.-M.; Perpéte, E. A. *J. Phys. Chem. A* **2006**, *110*, 5952−9.
(21) Jacquemin, D.; Femenias, A.; Chermette, H.; André, J.-M.; Perpète, E. A. *J. Phys. Chem. A* **2005**, *109*, 5734−41.
(22) Pople, J. A. *Proc. R. Soc. London, Ser. A* **1950**, *202*, 323.
(23) Casula, M.; Sorella, S. *J. Chem. Phys.* **2003**, *119*, 6500.
(24) Pauling, L. *The Nature of the Chemical Bond*, 3rd ed.; Cornell University Press, Itaca, NY, 1960; pp 230−240.
(25) Zen, A.; Coccia, E.; Luo, Y.; Sorella, S.; Guidoni, L. *J. Chem. Theory Comput.* **2014**, *10*, 1048−1061.
(26) Marchi, M.; Azadi, S.; Casula, C.; Sorella, S. *J. Chem. Phys.* **2009**, *131*, 154116.
(27) Valiev, M.; Bylaska, E.; Govind, N.; Kowalski, K.; Straatsma, T.; Dam, H. V.; Wang, D.; Nieplocha, J.; Apra, E.; Windus, T.; de Jong, W. *Comput. Phys. Commun.* **2010**, *181*, 1477−1489.
(28) (a) Foulkes, W. M. C.; Mitas, L.; Needs, R. J.; Rajagopal, G. *Rev. Mod. Phys.* **2001**, *73*, 33−83. (b) Kolorenč, J.; Mitas, L. *Rep. Prog. Phys.* **2011**, *74*, 026502.
(29) Sorella, S.; Casula, M.; Rocca, D. *J. Chem. Phys.* **2007**, *127*, 14105.
(30) Zen, A.; Luo, Y.; Sorella, S.; Guidoni, L. *J. Chem. Theory Comput.* **2013**, *9*, 4332−4350.
(31) Sorella, S.; Capriotti, S. *J. Chem. Phys.* **2010**, *133*, 234111.
(32) Barborini, M.; Sorella, S.; Guidoni, L. *J. Chem. Theory Comput.* **2012**, *8*, 1260−1269.
(33) Attaccalite, C.; Sorella, S. *Phys. Rev. Lett.* **2008**, *100*, 114501.
(34) Coccia, E.; Chernomor, O.; Barborini, M.; Sorella, S.; Guidoni, L. *J. Chem. Theory Comput.* **2012**, *8*, 1952−1962.
(35) Zen, A.; Luo, Y.; Mazzola, G.; Guidoni, L.; Sorella, S. *J. Chem. Phys.* **2015**, Submitted.
(36) (a) Casula, M.; Filippi, C.; Sorella, S. *Phys. Rev. Lett.* **2005**, *95*, 100201. (b) Casula, M.; Moroni, S.; Sorella, S.; Filippi, C. *J. Chem. Phys.* **2010**, *135*, 154113.
(37) Sorella, S. TurboRVB Quantum Monte Carlo package (accessed date October 12, 2013). http://people.sissa.it/~sorella/web/index.html.
(38) Marchi, M.; Azadi, S.; Sorella, S. *Phys. Rev. Lett.* **2011**, *107*, 086807.
(39) Neuscamman, E. *Phys. Rev. Lett.* **2012**, *109*, 203001.
(40) Horsch, P. *Phys. Rev. B* **1981**, *24*, 7351−7360.
(41) Baeriswyl, D.; Maki, K. *Phys. Rev. B* **1985**, *31*, 6633−6642.
(42) Sterpone, F.; Spanu, L.; Ferraro, L.; Sorella, S.; Guidoni, L. *J. Chem. Theory Comput.* **2008**, *4*, 1428−1434.
(43) Burkatzki, M.; Filippi, C.; Dolg, M. *J. Chem. Phys.* **2007**, *126*, 234105.
(44) Page, C. S.; Olivucci, M. *J. Comput. Chem.* **2003**, *24*, 298−309.
(45) Jacquemin, D.; Perpète, E. A.; Scalmani, G.; Frisch, M. J.; Kobayashi, R.; Adamo, C. *J. Chem. Phys.* **2007**, *126*, 144105.
(46) Shen, J.; Fang, T.; Li, S. In *Advances in the Theory of Atomic and Molecular Systems*; Piecuch, P., Maruani, J., Delgado-Barrio, G., Wilson, S., Eds.; Springer: Netherlands, 2009; Progress in Theoretical Chemistry and Physics Vol. *19*; pp 241−255.
(47) Taube, A. G.; Bartlett, R. J. *J. Chem. Phys.* **2008**, *128*, 044110.
(48) Zen, A.; Trout, B. L.; Guidoni, L. *J. Chem. Phys.* **2014**, *141*, 014305.
(49) Karton, A.; Ruscic, B.; Martin, J. M. *J. Mol. Struct.: THEOCHEM* **2007**, *811*, 345−353.
(50) Kuchitsu, K. *J. Chem. Phys.* **1968**, *49*, 4456−4462.
(51) Martin, J. M. L.; Taylor, P. R. *Chem. Phys. Lett.* **1996**, *248*, 336−344.
(52) Chase, M. W.; Davis, C. A.; Downey, J. R.; Frurip, D. J.; McDonald, R. A.; Syveru, A. N. *J. Phys. Chem. Ref. Data* **1986**, *14*, 1483.
(53) Kuchitsu, K. *J. Chem. Phys.* **1966**, *44*, 906.
(54) Duncan, J. *Mol. Phys.* **1974**, *28*, 1177−1191.
(55) Harmony, M. D.; Laurie, V. W.; Kuczkowski, R. L.; Schwendeman, R. H.; Ramsay, D. A.; Lovas, F. J.; Lafferty, W. J.; Maki, A. G. *J. Phys. Chem. Ref. Data* **1979**, *8*, 619−722.
(56) Roberto-Neto, O.; Chakravorty, S.; Machado, F. B. *J. Mol. Struct.: THEOCHEM* **2002**, *586*, 29−34.
(57) Duncan, J.; McKean, D.; Bruce, A. *J. Mol. Spectrosc.* **1979**, *74*, 361−374.

DOI: 10.1021/ct501157f
J. Chem. Theory Comput. 2015, 11, 508−517